Selective accumulation of photosensitizers in glioma with this malignancy through folate-carrier protein SLC46A1 in vitro and specimen

筑　波　大　学

博 士 （ 医 学 ） 学 位 論 文

Selective accumulation of photosensitizers in glioma with this malignancy through folate-carrier protein SLC46A1 in vitro and specimen

（グリオーマの悪性度に依存した SLC46A1 を介する光感受性物質の集積）

２０１３

筑波大学大学院博士課程人間総合科学研究科
高田智也

Introduction

Malignant glioma has a poor prognosis despite a combination of treatments that include surgery, radiotherapy and chemotherapy. The median survival time of patients with glioblastoma is only 14.6 months despite the combination of radiotherapy at 60 Gy for over 6 weeks and temozolomide following removal of the malignant glioma.[1] This poor prognosis is in part due to its radiochemoresistance and infiltrative tumor growth. To improve the prognosis, this malignant glioma requires cytoreductive surgery[2] without injury to normal tissues.

Perioperative fluorescence imaging (photodynamic diagnosis, PDD) has been applied for decades in an effort to enhance this surgery.[3-11] Tumor fluorescence derived from 5-aminolevulinic acid (5-ALA) contributes to improving the complete resection rate (from 36% to 65%), as well as increasing the rate of 6-month progression-free survival after surgery (from 21% to 41%).[4, 5] 5-ALA is an intermediate of the heme biosynthesis pathway. In many tumor cells, including glioblastoma, an excess of the exogenous pro-drug ALA results in the accumulation of protoporphyrin IX (PpIX), most likely due to low ferrochelatase activity.[12, 13] However, some mechanisms of tumor-specific fluorescence (such as the fundamentals of PDD) are not clear. Although porphyrins such as hematoporphyrin derivative (HpD)[14-16] or talaporfin sodium[17] show tumor-specific accumulation, the mechanism of this is not well known.

Recently, we reported on the proton-coupled folate transporter (PCFT) SLC46A1, which was originally identified as heme carrier protein 1 (HCP-1)[18] and upregulates the cellular uptake of HpD. SLC46A1 is expressed in cancer cells such as rat gastric cancer-like cells (RGK), human gastric cancer cells (AGS), human lung cancer cells (A549) and human uterine cervical carcinoma cells (HeLa), but not in rat normal gastric mucosal cells.[19] The expression of SLC46A1 could be an important factor for developing photodiagnosis and photodynamic therapy.

SLC46A1 is expressed mainly in the duodenum or kidney, in the liver in response to hypoxia and in the brain (though here only to a small degree at the choroid plexus).[20] SLC46A1 expression in glioma has not been reported, and no relationship with its malignancy grade has been shown.

In this study, we investigated the expression of SLC46A1 in surgical specimens and cell lines of glioma by immunohistochemistry and reverse transcription-PCR (RT-PCR). We also clarified the relationship between SLC46A1 and fluorescence intensity (HpD uptake) in vitro by RT-PCR and a cellular uptake assay.

Materials and methods

Immunohistochemistry

Following an institutional review board-approved protocol, formalin-fixed tumor samples were obtained from 24 cases of glioma. The definitive diagnosis of each sample was made from paraffin-embedded material according to the WHO 2007 guidelines (9 cases of WHO grade IV, 9 cases of grade III and 6 cases of grade II) (Fig. 1B).

The DAKO LSAB Kit for mouse and rabbit primary antibody (DAKO, Glostrup, Denmark) was used. Tissue sections were deparaffinized and incubated with 10% normal goat serum in phosphate-buffered saline (PBS) for 20 min. Sections were heated in TE buffer (pH 9.0) in a microwave oven for 10 min, incubated until they reached room temperature and then washed in flowing water. Intracellular peroxidase deficiency was created by immersing the sections in 0.3% hydrogen peroxide-containing methanol for 20 min. After two washes with PBS, the sections were reacted with primary antibody (rabbit polyclonal HCP-1: Abcam, Plc.) in 1% bovine serum

albumin in PBS at 4°C overnight. Immunostained sections were further stained using the Dako LSAB2 kit (Dako Japan Co., Tokyo, Japan) according to the manufacturer's guidelines. Immunoperoxidase staining was stopped after a certification of stained color. Nuclei were stained with hematoxylin, and the specimens were mounted in an encapsulating agent. The intracellular SLC46A1 immunostaining was assessed using a semiquantitative scale (0: not detected; 1: weak; 2: moderate; 3: strong) (Fig. 1A). The number of nuclei positive for the MIB-1 labeling index was determined by counting at least 1,000 tumor cells.

Cell culture

The human glioblastoma cell lines U87 and U251 were obtained from the American Type Culture Collection (Rockville, MD), and T98G cells were obtained from the RIKEN cell bank. U251 cells were cultured in DMEM (Life Technologies Co., Carlsbad, CA), and U87 and T98G cells were cultured in DMEM with high glucose at 37°C under 5% CO_2. These media contained 10% inactivated fetal bovine serum (FBS, Life technologies) and 1% penicillin/streptomycin (Life technologies).

RT-PCR

RT-PCR was performed according to the manufacturers' guidelines. Briefly, extracts from cells and specimens were obtained using a cell lysis buffer. Because the cDNAs were collected with SuperScript III kits (Invitrogen, Carlsbad, CA), RT-PCR was performed in 35 cycles (94°C for 30 sec, 50°C for 30 sec, 72°C for 30 sec). The SLC46A1 (HCP-1) primers were reverse, 5'- GGT AGA GTG AGT TGA AGA TG-3', and forward, 5'- CTG GAC CCT CTA CAT GAA CG-3'. The ß-actin primers were reverse, 5'-GGAGTTGAAGGTAGTTTCGTG-3', and forward, 5'-CGGGAAATCGTGCGTGACAT-3'. The predicted size of the amplified ß-actin DNA product

was 214 bp. The PCR products of 471/992 bp corresponded to SLC46A1.[21] The RT-PCR products were electrophoresed in 2% agarose gels for 30 min. The intensity of the band area in electrophoresed gels was measured in ImageJ software (National Institutes of Health, MA).

The amounts of cellular uptake of HpD

In a 6-well dish, 1×10^6 cells were incubated for 24 h. Then, 0.1 mM of HpD (Wako Pure Chemical Ind., Osaka, Japan) was added to cells at 37°C for 1 and 3 h under light shielding. HpD was extracted from the cells by adding 500 μL of dimethyl sulphoxide (Wako Pure Chemical) after two washes with cold PBS. The extracts were centrifuged for 10 min at 10,000 rpm, and 100-μL supernatants were collected. The fluorescence intensities of the 100-μL supernatants in a 96-well plate were measured by a micro plate reader (Ex. 415 nm, Em. 625 nm) (Varioskan; Thermo Fisher Scientific K.K., Kanagawa, Japan).

HpD fluorescence imaging

In 35-mm glass dishes, 5×10^5 cells were incubated for 24 h, then treated with 0.1 mM HpD at 37°C for 1 or 3 h. After the cells were washed twice with cold PBS, the fluorescence image was captured using a fluorescence microscope system (Biozero; Keyence Co., Tokyo, Japan).

Statistical analysis

The statistical analysis was performed using KaleidaGraph software (HULINKS Inc., Tokyo, Japan). Statistical significance (p value) was calculated using ANOVA followed by Scheffe's F-test.

Results

SLC46A1 expression in glioma surgical specimens

Figure 1 shows the clinical features and SLC46A1 expression as observed by immunohistochemistry of 24 glioma cases. The immunostained specimens were classified into four groups based on the expression of SLC46A1: not detected (Fig. 1A, 0), weak (Fig. 1A, 1), moderate (Fig. 1A, 2) and strong (Fig. 1A, 3). SLC46A1 expression was observed in all specimens: 25% presented strong expression, 71% presented moderate expression, and 4% presented weak expression (Fig. 1B, SLC46A1). Additionally, 67% of the highly fluorescent specimens in the intraoperative PDD strongly expressed SLC46A1 (Fig. 1B, PDD). Regarding the malignancy grades, 33% of the grade IV specimens, 22% of the grade III specimens and 17% of the grade II specimens strongly expressed SLC46A1 (Fig. 1B, grade and SLC46A1). The expression of SCL46A1 in the specimens appeared to coincide with malignancy. For further specific evidence of SLC46A1 expression in malignant tissue, Fig. 2 shows a slice including an area of both malignant tissue and normal tissue. SLC46A1 was only expressed in the malignant area.

To confirm SLC46A1 expression of malignant glioma, we randomly chose four frozen sections (2 cases of grade III, 2 cases of grade IV); all four strongly expressed SLC46A1 mRNA (by RT-PCR) (Fig. 3).

SLC46A1-expressing and cellular uptake of HpD

The expression of SLC46A1 in U87, U251 and T98G cells was determined by RT-PCR. SLC46A1 showed different levels of expression in each cell line, increasing in the order U87 (no SLC46A1 mRNA) to U251 to T98G (Fig. 4).

Fig. 5 shows the cellular uptake of HpD by U87, U251 and T98G. The amount of HpD in the cells increased in the order U87 to U251 to T98G. While the HpD fluorescence images showed slight differences in cellular uptake (Fig. 5A), the HpD fluorescence intensity showed significant differences (Fig. 5B). The HpD fluorescence intensity in T98G was 2.8-fold greater than that in U87.

The amounts of HpD cellular uptake coincided with SLC46A1 expression. These results suggest that the accumulation of HpD in glioma cells is related to the expression of SLC46A1.

Discussion

In this study, proton-coupled folate transporter SLC46A1 expression was quantified in surgical specimens and in glioma cell lines. Our findings indicate that the expression of SLC46A1 coincides with HpD cellular uptake, and SLC46A1 seems to be related to the malignancy grade of glioma. In our previous study, SLC46A1 was expressed in gastric cancer cells but not in normal gastric cells.[19] These results suggest that SLC46A1 could become an indicator of malignant area. In addition, the current study and our previous study suggest that selective accumulation of HpD in the tumor is dependent on SLC46A1.

Talaporfin sodium is a new photosensitizer for photodynamic therapy (PDT) in the lung.[22] The clinical application of PDT will be expanded to other tissues in the near future.[22, 23] For the treatment of malignant glioma, talaporfin sodium has progressed to a phase II clinical study, and the safety and therapeutic effects of talaporfin have been reported.[24-27] While talaporfin sodium and HpD are porphyrin structure, SLC46A1 probably transports talaporfin sodium as well as HpD through structural recognition.[28] In a vasogenic edema model, 5-ALA did not increase fluorescence intensity in the contralateral brain, but talaporfin did.[17] An area of edema is thought

to undergo oxidative stress and could lead to talaporfin sodium accumulation in an area through SLC46A1. This phenomenon could make it difficult to distinguish the invaded area from a peritumoral edema. This could be a limitation of talaporfin sodium PDD.

SLC46A1 is a porphyrin and folic acid transporter in the human duodenum and is regulated in hypoxia[18]. Porphyrin and folic acid are necessary to maintain cellular homeostasis through the activity of redox enzymes and the synthesis both DNA and amino acids, respectively.[28] Because mitochondrial complex I and mitochondrial complex III dysfunction are critical in cancer cells, an electron transfer system easily generates reactive oxygen species (ROS).[29, 30] Consequently, cancer cells are often oxidatively stressed. This stress causes harmful effects such as lipid peroxidation and apoptosis via DNA damage.[31, 32] Activities of redox and DNA repair protect from this stress; thus, cancer cells should require antioxidants and the material required for DNA repair for its survival. The intracellular antioxidant of manganese superoxide dismutase is more abundant in normal cells than cancer cells.[33] These factors may explain the expression of SLC46A1 in malignant cells. If we could control the expression of SLC46A1, especially silencing SLC46A1 in tumor cells, transportation of porphyrin or folic acid could be selectively controlled. This process has the potential to become the key to a new molecular targeting therapy.

Conclusion

Proton-coupled folate transporter SLC46A1 expression was measured in surgical specimens and glioma cell lines. SLC46A1 is involved in the mechanism of glioma fluorescence.

Acknowledgements

We gratefully acknowledge Yoshiko Tsukada and Makiko Miyakawa for their excellent technical assistance. This study was partially supported by the project of KAKEN (23659576).

Conflict of interest

No conflict of interest exists.

References

1. Stupp R, Mason WP, van den Bent MJ, *et al.* Radiotherapy plus concomitant and adjuvant temozolomide for glioblastoma. *N Engl J Med* 2005; **352**: 987-996.

2. Stummer W, van den Bent MJ, Westphal M. Cytoreductive surgery of glioblastoma as the key to successful adjuvant therapies: new arguments in an old discussion. *Acta Neurochir (Wien)* 2011; **153**: 1211-1218.

3. Eljamel MS. Photodynamic assisted surgical resection and treatment of malignant brain tumours technique, technology and clinical application. *Photodiagnosis Photodyn Ther* 2004; **1**: 93-98.

4. Stummer W, Pichlmeier U, Meinel T, *et al.* Fluorescence-guided surgery with 5-aminolevulinic acid for resection of malignant glioma: a randomised controlled multicentre phase III trial. *Lancet Oncol* 2006; **7**: 392-401.

5. Stummer W, Novotny A, Stepp H, *et al.* Fluorescence-guided resection of glioblastoma multiforme utilizing 5-ALA-induced porphyrins: a prospective study in 52 consecutive patients. *J Neurosurg* 2000; **93**: 1003-1013.

6. Novotny A, Xiang J, Stummer W, *et al.* Mechanisms of 5-aminolevulinic acid uptake at the choroid plexus. *J Neurochem* 2000; **75**: 321-328.

7. Schmidt MH, Bajic DM, Reichert KW, *et al.* Light-emitting diodes as a light source for intraoperative photodynamic therapy. *Neurosurgery* 1996; **38**: 552-557.

8. Yang VX, Muller PJ, Herman P, *et al.* A multispectral fluorescence imaging system: Design and initial clinical tests in intra-operative Photofrin-photodynamic therapy of brain tumors. *Lasers Surg Med* 2003; **32**: 224-232.

9. Lilge L, Wilson BC. Photodynamic therapy of intracranial tissues: a preclinical comparative study of four different photosensitizers. *J Clin Laser Med Surg* 1998; **16**: 81-91.

10. Kostron H, Bellnier DA, Lin CW, *et al.* Distribution, retention, and phototoxicity of hematoporphyrin derivative in a rat glioma. Intraneoplastic versus intraperitoneal injection. *J Neurosurg* 1986; **64**: 768-774.

11. Eljamel MS, Goodman C, Moseley H. ALA and Photofrin fluorescence-guided resection and repetitive PDT in glioblastoma multiforme: a single centre Phase III randomised controlled trial. *Lasers Med Sci* 2008; **23**: 361-367.

12. Karmakar S, Banik NL, Patel SJ, *et al.* 5-Aminolevulinic acid-based photodynamic therapy suppressed survival factors and activated proteases for apoptosis in human glioblastoma U87MG cells. *Neurosci Lett* 2007; **415**: 242-247.

13. Teng L, Nakada M, Zhao S, *et al.* Silencing of ferrochelatase enhances 5-aminolevulinic acid-based fluorescence and photodynamic therapy efficacy. *Br J Cancer* 2011; **104**: 798-807

14. Kessel D, Chou T-H. Tumor-localizing components of the porphyrin preparation hematoporphyrin derivative. *Cancer Res* 1983; **43**: 1994-1999.

15. Bugelski PJ, Porter CW, Dougherty TJ. Autoradiographic distribution of hematoporphyrin derivative in normal and tumor tissue of the mouse. *Cancer Res* 1981; **41**: 4606-4612.

16. Kessel D, Cheng M-L. Biological and biophysical properties of the tumor-localizing component of hematoporphyrin derivative. *Cancer Res* 1985; **45**: 3053-3057.

17. Tsurubuchi T, Zoboronok A, Yamamoto T, *et al.* The optimization of fluorescence imaging of brain tumor tissue differentiated from brain edema—In vivo kinetic study of 5-aminolevulinic acid and talaporfin sodium. *Photodiagnosis Photodyn Ther* 2009; **6**: 19-27.

18. Shayeghi M, Latunde-Dada GO, Oakhill JS, *et al.* Identification of an intestinal heme transporter. *Cell* 2005; **122**: 789-801.

19. Hiyama K, Matsui H, Tamura M, *et al.* Cancer cells uptake porphyrins via heme carrier protein 1. *J Porphyrins Phthalocyanines* 2013; **17**: 36-43.

20. Qiu A, Jansen M, Sakaris A, *et al.* Identification of an intestinal folate transporter and the molecular basis for hereditary folate malabsorption. *Cell* 2006; **127**: 917-928.

21. Gonen N, Assaraf YG. The obligatory intestinal folate transporter PCFT (SLC46A1) is regulated by nuclear respiratory factor 1. *Journal of Biological Chemistry* 2010; **285**: 33602-33613.

22. Nanashima A, Abo T, Nonaka T, *et al.* Photodynamic Therapy Using Talaporfin Sodium (Laserphyrin®) for Bile Duct Carcinoma: A Preliminary Clinical Trial. *Anticancer Res* 2012; **32**: 4931-4938.

23. Nonaka Y, Nanashima A, Nonaka T, *et al.* Synergic effect of photodynamic therapy using talaporfin sodium with conventional anticancer chemotherapy for the treatment of bile duct carcinoma. *J Surg Res* 2013; **181**: 234-241.

24. Muragaki Y, Akimoto J, Maruyama T, *et al.* Phase II clinical study on intraoperative photodynamic therapy with talaporfin sodium and semiconductor laser in patients with malignant brain tumors. *J Neurosurg* 2013; **119**: 845-852.

25. Tsutsumi M, Miki Y, Akimoto J, *et al.* Photodynamic therapy with talaporfin sodium induces dose-dependent apoptotic cell death in human glioma cell lines. *Photodiagnosis Photodyn Ther* 2013; **10**: 103-110.

26. Yano T, Muto M, Yoshimura K, *et al.* Phase I study of photodynamic therapy using talaporfin sodium and diode laser for local failure after chemoradiotherapy for esophageal cancer. *Radiat Oncol* 2012; **7**: 113.

27. Akimoto J, Haraoka J, Aizawa K. Preliminary clinical report on safety and efficacy of photodynamic therapy using talaporfin sodium for malignant gliomas. *Photodiagnosis Photodyn Ther* 2012; **9**: 91-99.

28. Krishnamurthy P, Xie T, Schuetz JD. The role of transporters in cellular heme and porphyrin homeostasis. *Pharmacol Ther* 2007; **114**: 345-358.

29. Guzy RD, Hoyos B, Robin E, *et al.* Mitochondrial complex III is required for hypoxia-induced ROS production and cellular oxygen sensing. *Cell metabolism* 2005; **1**: 401-408.

30. Taddei ML, Giannoni E, Raugei G, *et al.* Mitochondrial oxidative stress due to complex I dysfunction promotes fibroblast activation and melanoma cell invasiveness. *J Signal Transuct* 2012; **2012**: 684592.

31. Cook JA, Gius D, Wink DA, *et al.* Oxidative stress, redox, and the tumor microenvironment. *Semin Radiat Oncol* 2004; **14**: 259-266.

32. Singh A, Rangasamy T, Thimmulappa RK, *et al.* Glutathione peroxidase 2, the major cigarette smoke–inducible isoform of GPX in lungs, is regulated by Nrf2. *Am J Respir Cell Mol Biol* 2006; **35**: 639.

33. Tamura, M. *et al.* Mitochondrial reactive oxygen species accelerated gastric cancer cellular invasion. *J Clin Biochem Nutr* 2013; **in press**.

Figure Legends

Figure 1. Information on the malignancy grade of specimens and the expression of SLC46A1. (A) The expression level of SLC46A1 expressions from immunostained specimens. The intracellular SLC46A1 immunostaining was assessed using a semiquantitative scale (0: not detected; 1: weak; 2: moderate; 3: strong). Nuclei positive for MIB-1 were determined by counting at least 1,000 tumor cells. (B) 24 cases of clinical indications and SLC46A1 expression according to the upper images. The malignancy grade was based on the 2007 WHO classification of tumors of the central nervous system. GBM: glioblastoma; GBMO: glioblastoma with oligodendroglial component; AA: anaplastic astrocytoma; AOD: anaplastic oligodendroglioma; AOA: anaplastic oligoastrocytoma; OD: oligodendroglioma; OA: oligoastrocytoma; PXA: pleomorphic xanthoastrocytoma; lt: left; rt: right; F: frontal lobe; T: temporal lobe; P: parietal lobe; O: occipital lobe; lat. vent.: lateral ventricle

Figure 2. Tissue immunostained for SLC46A1 protein. While the malignant tumor area (upper area) was stained with antibody against SLC46A1, the normal area (bottom area) was not stained with this antibody. (×200)

Figure 3. SLC46A1 mRNA expression in the specimens of four randomly selected cases of malignant glioma (G: grade) by RT-PCR.

Figure 4. mRNA expression in U87, U251 and T98G cells by RT-PCR. (A) Bands of SLC46A1 (182 bp) and β-actin (228 bp) in 2% agarose gel stained with ethidium bromide. (B) The relative intensity of the band area of SLC46A1 and β-actin in each cell line.

Figure 5. Cellular uptake of HpD in U87, U251 and T98G. Cellular uptake was determined by HpD fluorescence intensity and fluorescence images. (A) Fluorescence images. The cells were

incubated with 0.1 mM HpD at 37°C for 1 and 3 h. The fluorescence images were captured by fluorescence microscope. Scale bars: 50 μm (B) HpD fluorescence intensity. A total of 1×10^6 cells were incubated with 0.1 mM HpD at 37°C for 1 or 3 h. Then, 100 μL of the extracted HpD cells was measured using a plate reader (Em. 415 nm, Ex. 625 nm). HpD was then extracted from cells using DMSO. Error bars indicate standard deviation. Two-way analysis of variance (ANOVA) suggested a significant effect of cell type on the HpD concentration. Statistically significant differences were determined by employing Scheffe's F-test and are denoted as $^{**}p < 0.01$ (n=3).

(A)

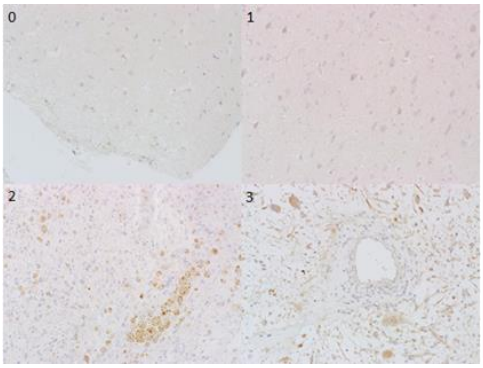

(B)

No.	age	gender	removal	pathology	grade	location	MIB-1(%)	SLC46A1	PDD
1	39	F	partial	GBM	Ⅳ	bi. F	32.3	3	1
2	46	M	subtotal	GBM	Ⅳ	lt. T	38.6	2	2
3	72	M	subtotal	GBM	Ⅳ	lt. F	12.6	3	3
4	65	F	partial	GBM	Ⅳ	lt. T	70.4	1	2
5	65	M	subtotal	GBM	Ⅳ	lt. P	33.7	2	3
6	61	M	partial	GBM	Ⅳ	lt. F-T	30.3	2	0
7	66	F	total	GBM	Ⅳ	rt. O	17.7	3	-
8	74	M	partial	GBMO	Ⅳ	rt. F	20	2	2
9	58	F	partial	GBMO	Ⅳ	bi. F	35.7	2	-
10	32	F	total	AA	Ⅲ	lt .F	17	2	-
11	61	F	partial	AOD	Ⅲ	lt. F	9.7	2	-
12	60	F	partial	AOD	Ⅲ	lt. T	9.6	2	-
13	73	M	subtotal	AOD	Ⅲ	lt. F	26	2	-
14	62	M	subtotal	AOA	Ⅲ	pineal	30.6	3	-
15	54	M	total	AOA	Ⅲ	lt. F	4.8	2	2
16	71	F	total	AOA	Ⅲ		27.4	2	-
17	28	F	total	AOA	Ⅲ	lt.F	8.5	2	1
18	33	F	total	AOA	Ⅲ	rt.F	8.4	3	3
19	41	M	subtotal	OD	Ⅱ	lt. lat. vent.	5	2	1
20	37	M	subtotal	OA	Ⅱ	rt.P	1.2	2	-
21	35	M	total	OA	Ⅱ	lt.F	1.9	3	-
22	41	M	subtotal	OA	Ⅱ	rt.F	2.4	2	-
23	42	M	total	OA	Ⅱ	rt.F	8	2	-
24	33	F	total	PXA	Ⅱ	lt.T	1.5	2	1

Figure 1

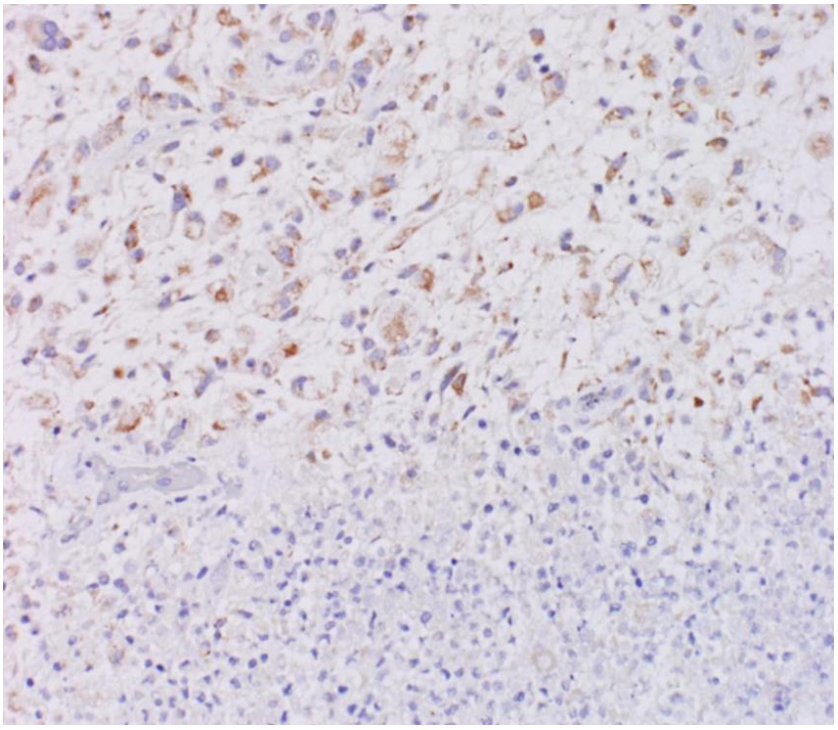

Figure 2

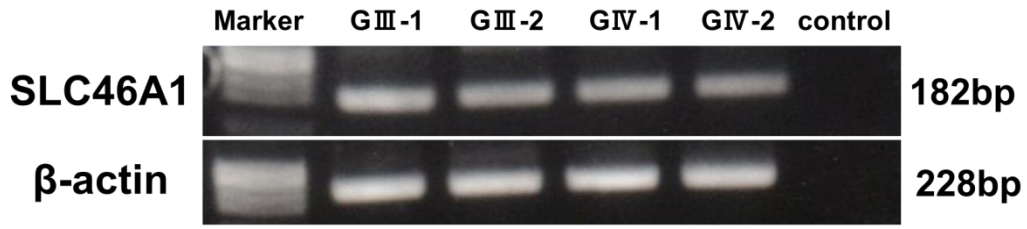

Figure 3

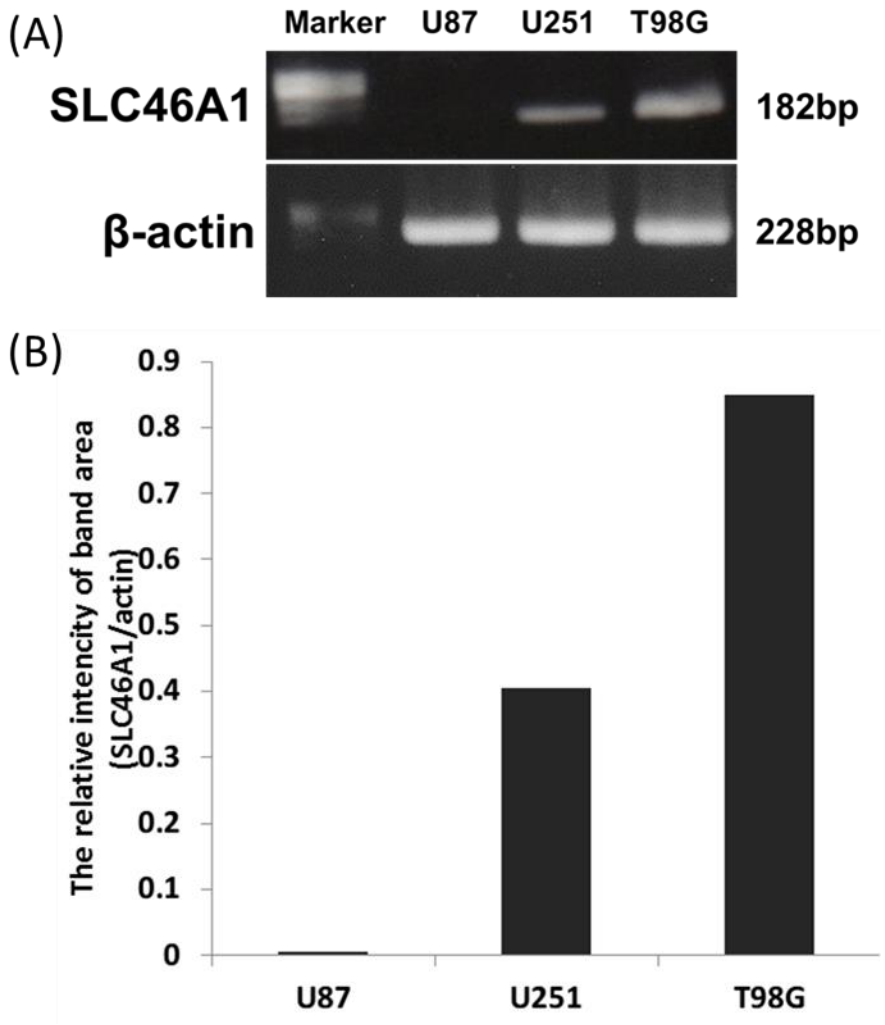
(A)
Marker
U87
U251
T98G
SLC46A1
182bp
β-actin
228bp
(B)
The relative intencity of band area (SLC46A1/actin)
0.9
0.8
0.7
0.6
0.5
0.4
0.3
0.2
0.1
0
U87
U251
T98G

Figure 4

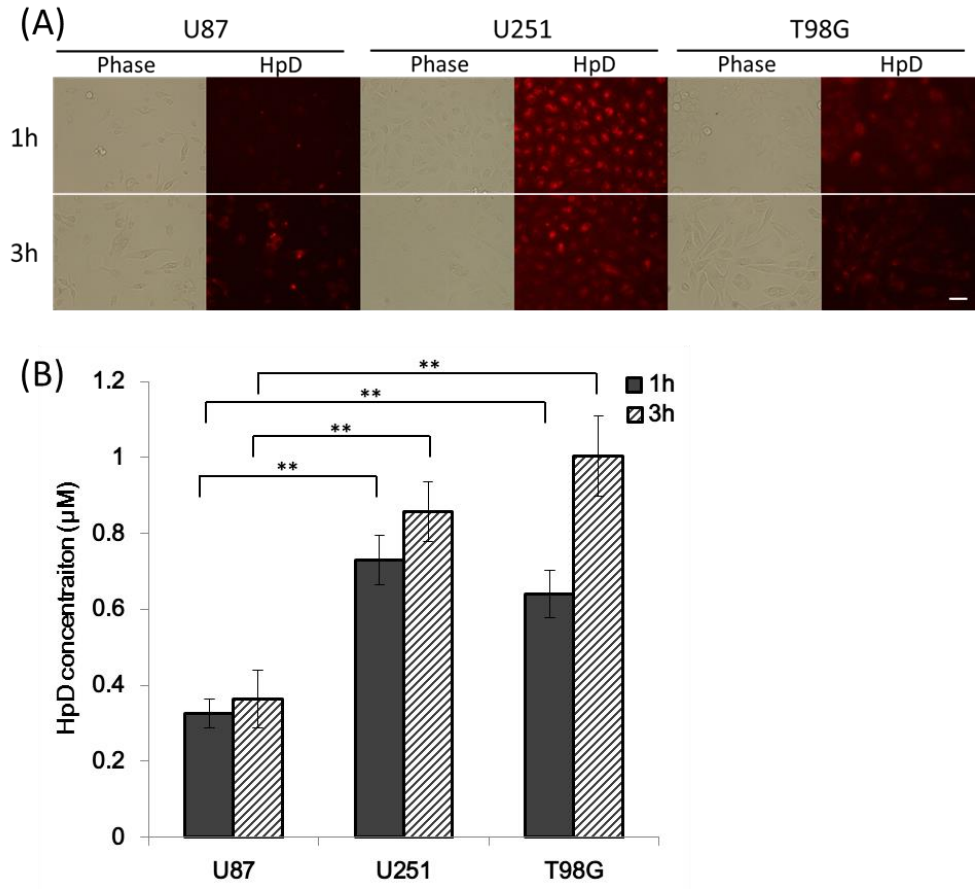
(A)
U87
U251
T98G
Phase
HpD
Phase
HpD
Phase
HpD
1h
3h
(B)
HpD concentraiton (μM)
1.2
1
0.8
0.6
0.4
0.2
0
**
**
**
**
1h
3h
U87
U251
T98G

Figure 5

謝辞

本稿を終えるにあたり、研究をご指導賜りました、筑波大学医学医療系脳神経外科松村明教授に深謝いたします。また、本研究について多くのご助言とご協力を賜りました、筑波大学医学医療系脳神経外科山本哲哉講師ならびに同消化器内科松井裕史講師をはじめ多くの諸先生方に感謝いたします。